# Pre-clinical characterization of the novel Fibroblast Activation Protein (FAP) targeting ligand PNT6555 for the imaging and therapy of cancer

*Robin M. Hallett[1], Sarah E. Poplawski[2], Kyle E. Novakowski[1], Mark H. Dornan[1], Shin Hye Ahn[3], Shuang Pan[2], Wu Wengen[2], Liu Yuxin[2], David G. Sanford[2], Valerie S. Hergott[1], Quang-De Nguyen[3], Anthony P. Belanger[3], Jack H. Lai[2], William W. Bachovchin[2], Joe A. B. McCann[1]*

*[1]POINT Biopharma Inc, Indianapolis, IN, [2]Tufts University, Boston, MA, [3]Dana-Farber Cancer Institute, Boston, MA*

**SNMMI AGM 2022**
**Abstract ID: 490**

## Introduction

### Fibroblast Activation Protein (FAP-α)

- Fibroblast Activation Protein-α (FAP-α) is a compelling pan cancer target for imaging and therapy as it is overexpressed in >90% of epithelial tumors[1].
- In cancer, FAP is highly expressed on cancer associated fibroblasts (CAFs)[2], which drive tumor progression and resistance to chemo and immunotherapy[3,4,5].
- FAP shows limited expression in adult normal tissues[6].
- FAP positivity based on FAP targeted PET imaging has been demonstrated in most common solid tumors[7].
- POINT Biopharma has developed PNT6555, a FAP-targeting small molecule with high selectivity for FAP, for the diagnosis and treatment of FAP-avid solid tumors.

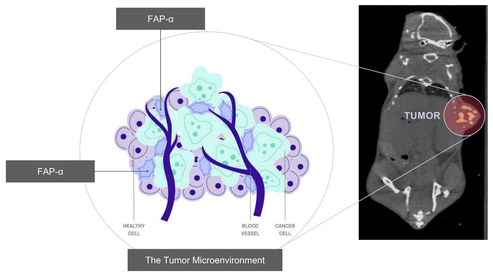


**Figure 1**: Schematic representation of the FAP-expressing CAFs in the tumor microenvironment.

### PNT6555

- PNT6555 comprises a DOTA chelator (1,4,7,10-tetraazacyclododecane-1,4,7,10- tetraacetic acid) and a FAP-targeting moiety (Bz-D-Ala-boroPro) connected via an aminomethyl linker.
- Gallium-68 is chelated to PNT6555 for diagnostic purposes and lutetium-177 or actinium-225 is chelated to PNT6555 for therapeutic purposes.

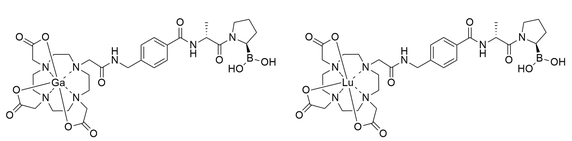

**Figure 2**: The corresponding (Ga/Lu-DOTA-AmBz-D-Ala-boroPro) chelates represent the imaging and therapeutic theranostic pair of PNT6555.

## Materials & Methods

- **Biochemistry:** Potency ($IC_{50}$) and enzyme specificity studies were performed using soluble FAP/DPP4/PREP derived from either recombinant protein or human serum. Murine FAP was expressed on HEK 293 cells (HEK-mFAP). FAP/DPP4/PREP inhibition was measured using fluorogenic FAP/DPP4/PREP substrates and measuring the release of the fluorescent cleavage product. Non-radioactive (natural) gallium and lutetium isotopes were used for all *in vitro* studies.
- **Animal experiments:** All animal experiments were approved by the Dana-Farber Cancer Institute Animal Care and Use Committee. For HEK-mFAP tumor xenograft studies, Male Fox Chase SCID mice were purchased from Charles River Laboratories at 6-8 weeks old and allowed to acclimate for 1 week. All mice were housed under standard care conditions and monitored weekly. Tumors were established by subcutaneous injection of 5 x $10^6$ cells into the right flank in 100 µL PBS.
- **Tumor growth:** Tumor growth was monitored weekly with caliper measurements (tumor volume = length × $width^2$ × 0.5). Study endpoints include tumor size > 2 cm in any dimension, tumor ulceration, mouse is moribund, and > 15% body weight lost from the last measurement.
- **PET/SPECT studies:** PET and SPECT imaging studies were performed using a dedicated small animal PET/CT / SPECT/CT scanner with animals under gaseous anesthesia. Following a 7.4 MBq bolus injection (IV) of $^{68}$Ga-PNT6555, Dynamic PET scans were performed in list mode format over 60 min, followed by image reconstruction in FORE/3D-OSEM-MAP. Low dose CT scans were performed for anatomical reference and to segment and extract volume of interest-derived standardized uptake values (SUVs).
- **Biodistribution studies:** Biodistribution studies were performed at defined time points following a 7.5 MBq bolus injection (IV) of 177Lu-PNT6555. Tissue samples were counted for radioactivity on a Cobra-II Auto-Gamma counter and data was expressed as injected dose per gram (%ID/g).
- **Efficacy:** Efficacy studies were performed using HEK-mFAP tumor bearing male Fox Chase SCID mice. Mice were treated with a single bolus (IV) injection of either $^{177}$Lu-PNT6555 or $^{225}$Ac-PNT6555 and monitored for tumor volume and survival.

## Results

### PNT6555 potently and specifically inhibits FAP

- PNT6555, cold Ga-labelled PNT6555 and cold Lu-labelled PNT6555 potently inhibited FAP (Table 1).
- A high degree of specificity for FAP was also demonstrated for PNT6555 as compared to the related enzymes PREP and DPP4 (Table 2).

**Table 1:** Potency of PNT6555 and $^{nat}$Lu/$^{nat}$Ga-PNT6555 on inhibition of human FAP.

| | Recombinant Human FAP | Human Serum FAP | HEK-mFAP |
|---|---|---|---|
| **Inhibitor** | **$IC_{50}$ (nM)** | **$IC_{50}$ (nM)** | **$IC_{50}$ (nM)** |
| PNT6555 | 1.8 ± 0.4 | 2.5 ± 0.4 | 0.8 ± 0.03 |
| $^{nat}$Lu-PNT6555 | 6.6 ± 0.5 | 10 ± 1.7 | 1.2 ± 0.1 |
| $^{nat}$Ga-PNT6555 | 98 ± 5.4 | 100 ± 9.3 | 47 ± 5.9 |

**Table 2:** Selectivity indices of PNT6555 and $^{nat}$Lu/$^{nat}$Ga-PNT6555 on inhibition of PREP and DPPIV.

| | PREP | DPP4 |
|---|---|---|
| **Inhibitor** | **Selectivity Index** | **Selectivity Index** |
| PNT6555 | 500 | >55000 |
| $^{nat}$Lu-PNT6555 | 621 | >15000 |
| $^{nat}$Ga-PNT6555 | 37 | >10000 |

### *In vivo* biodistribution of $^{68}$Ga-PNT6555

- Based on SUVmean, $^{68}$Ga-PNT6555 uptake in the blood of tumor-bearing mice peaked at 4.3 (SEM: 0.26) at 0.375 min post-injection and subsequently showed a continuous decrease throughout the imaging interval to 0.3 (SEM 0.03) at 57.5 min.
- In tumor-bearing mice, kidney uptake peaked at 3.84 (SEM 1.02) at 2.5 min post-injection and decreased to 0.76 (SEM 0.01) at 57.5 min.
- The tumor was the only tissue of increasing uptake throughout the imaging interval, with very limited uptake into normal tissues and rapid clearance through the kidneys and into the bladder.

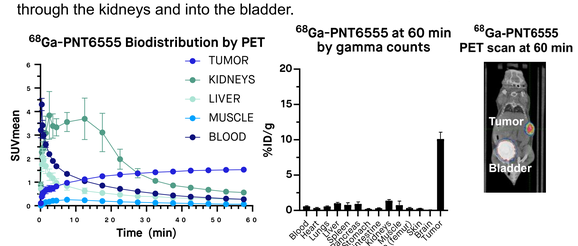


**Figure 3:** (Left) Biodistribution of $^{68}$Ga-PNT6555 in HEK-mFAP tumor-bearing mice was assessed by dynamic PET imaging. (Middle) Direct organ assay by gamma-counting in tissues collected at 60 min necropsy. (Right) PET image taken at 60 min.

### *In vivo* biodistribution of $^{177}$Lu-PNT6555

- **SPECT:** $^{177}$Lu-PNT6555 was cleared rapidly through the kidneys into the bladder, with significant activity observed in the bladder at 3h (35.76 %ID/mL, SEM: 9.45) and 24h (3.4 %ID/mL, SEM: 1.84).
- **Biodistribution:** Very limited retention was observed in normal tissues. Tumor showed prolonged retention out to 168h (11.41 %ID/g, SEM: 1.71).

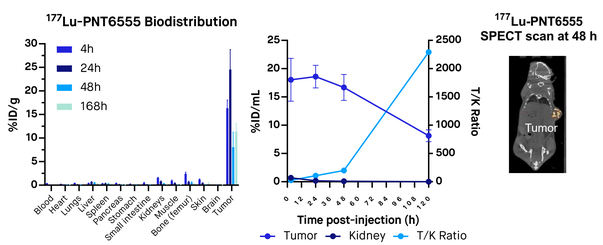


**Figure 4:** (Left) Biodistribution of $^{177}$Lu-PNT6555 by direct organ assay in HEK-mFAP tumor-bearing mice in tissues collected at indicated timepoints. (Middle) Tissue distribution assessed by SPECT imaging in tumor and kidney tissues and the tumor:kidney ratio of %ID/mL across the experimental time course. (Right) SPECT image taken at t=48h.

## Results (*Ctd.*)

### *In vivo* biodistribution of $^{177}$Lu-PNT6555 (*Ctd.*)

- **Biodistribution:** Rapid time-dependent clearance of $^{177}$Lu-PNT6555 from all normal tissues in tumor-free mice was observed. The tissues with the highest level of activity were whole bone (1.95% ID/g at 4 h, SEM 0.18) and uterus (1.69% ID/g at 4 h, SEM 0.33). Activity within whole bone decreased to 0.40% ID/g (SEM 0.04) at 168 h and activity within uterus decreased to 0.63% ID/g (SEM 0.29) at 168 h post-injection.

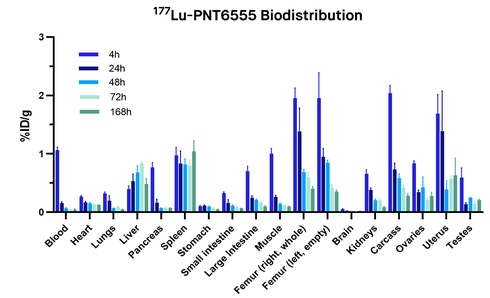


**Figure 5:** Biodistribution of 177Lu-PNT6555 in male and female Fox Chase SCID mice was assessed by direct organ assay by gamma-counting in tissues collected at the indicated time points.

### Human Radiation Dosimetry Estimates for $^{68}$Ga-PNT6555 and $^{177}$Lu-PNT6555

- Human dosimetry estimates for $^{68}$Ga-PNT6555 based on biodistribution data from HEK-mFAP tumor-bearing mice determined that the organs receiving the largest absorbed doses were the urinary bladder wall (0.39 mGy/MBq in males, 0.49 mGy/MBq in females) and uterus (0.030 mGy/MBq).
- Human dosimetry estimates for $^{177}$Lu-PNT6555 based on biodistribution data from tumor-free mice determined that the organs receiving the largest absorbed doses were the urinary bladder wall (0.40 mGy/MBq in males, 0.52 mGy/MBq in females) and osteogenic cells (0.21 mGy/MBq in males, 0.19 mGy/MBq in females).

**Table 3:** Human dosimetry estimates of $^{68}$Ga-PNT6555 in tumor-bearing mice and $^{177}$Lu-PNT6555 in tumor-free mice, by organ

| | $^{68}$Ga-PNT6555 | | $^{177}$Lu-PNT6555 | |
|---|---|---|---|---|
| | **Males (mGy/MBq)** | **Females (mGy/MBq)** | **Males (mGy/MBq)** | **Females (mGy/MBq)** |
| Adrenals | 0.012 | 0.014 | 0.092 | 0.10 |
| Brain | 0.0098 | 0.012 | 0.0022 | 0.0026 |
| Small Intestine | 0.015 | 0.018 | 0.022 | 0.026 |
| Heart Wall | 0.011 | 0.014 | 0.0092 | 0.011 |
| Kidneys | 0.012 | 0.015 | 0.010 | 0.012 |
| Liver | 0.0058 | 0.0072 | 0.026 | 0.032 |
| Red Marrow | 0.011 | 0.014 | 0.057 | 0.069 |
| Osteogenic Cells | 0.0099 | 0.010 | 0.21 | 0.19 |
| Spleen | 0.011 | 0.014 | 0.041 | 0.051 |
| Urinary Bladder Wall | 0.39 | 0.49 | 0.40 | 0.52 |
| Uterus | N/A | 0.030 | N/A | 0.049 |
| Total Body | 0.013 | 0.016 | 0.027 | 0.033 |
| ED (mSv/MBq) | 0.024 | 0.032 | 0.037 | 0.050 |

- The biodistribution data from the animals were extrapolated to predict human biodistribution using relative organ mass scaling.
- Dosimetry estimates for target organs were produced using the RADAR/MIRD methods and/or OLINDA/EXM software.

## Results (*Ctd.*)

### *In vivo* efficacy of $^{177}$Lu-PNT6555

- Dose-dependent tumor regression was observed, with significant benefits to survival.
- 6/6 mice treated at 60 MBq and 3/6 mice treated at 30 MBq showed complete and durable tumor regression.
- Median survival was extended from 22 days in the precursor group to 54 days in the 15 MBq group. 30 MBq and 60 MBq groups did not reach median survival.

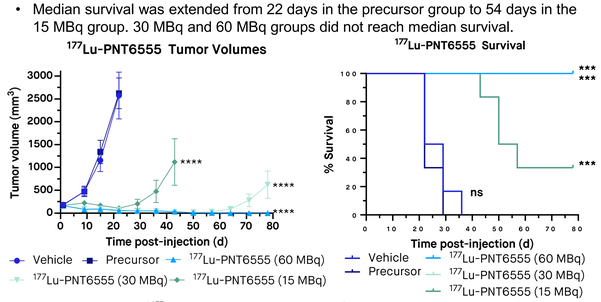


**Figure 6:** The capacity of $^{177}$Lu-PNT6555 to inhibit the growth of HEK-mFAP tumor-bearing mice. (Left) Tumor volume was determined until day 78 by weekly caliper measurements. Tumor volumes are shown until the first mouse reached endpoint. Statistical comparisons were performed on the date of the first mouse in the precursor group reaching endpoint (day 22). **** $p < 0.0001$, one way ANOVA. (Right) Survival curves are shown until day 78 post-injection. *** $p < 0.001$, Log-rank test.

### *In vivo* efficacy of $^{225}$Ac-PNT6555

- Dose-dependent tumor regression was observed, with significant increases in survival.
- 4/6 mice treated at 50 kBq showed complete and durable tumor regression.
- Median survival was extended from 19 days in the precursor group to 29 days in the 5 kBq group and 64 days in the 25 kBq group. The 50 kBq group did not reach median survival.

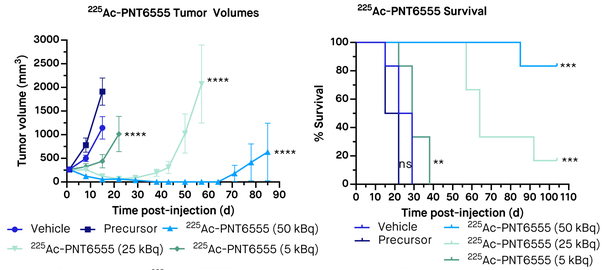


**Figure 7:** The capacity of $^{225}$Ac-PNT6555 to inhibit the growth of HEK-mFAP tumor-bearing mice. (Left) Tumor volume was determined until day 85 by weekly caliper measurements. Tumor volumes are shown until the first mouse reached endpoint. Statistical comparisons were performed on the date of the first mouse in the precursor group reaching endpoint (day 15), **** $p < 0.0001$, one way ANOVA. (Right) Survival curves are shown until day 104 post-injection. ** $p < 0.01$, *** $p < 0.001$, Log-rank test.

## Conclusions

- PNT6555 shows nanomolar potency against human and murine FAP and high selectivity over closely-related targets.
- In preclinical models, $^{68}$Ga-PNT6555 is an effective imaging agent, with strong tumor targeting, low background in normal tissues and rapid clearance via urinary excretion.
- $^{177}$Lu-PNT6555 shows prolonged tumor retention out to 168 h post-injection.
- Efficacy studies of $^{177}$Lu-PNT6555 and $^{225}$Ac-PNT6555 demonstrate compelling, dose-responsive inhibition of HEK-mFAP tumor growth.
- Clinical studies are planned using $^{68}$Ga-PNT6555 for imaging and $^{177}$Lu-PNT6555 for therapy.

## References

**1.** Mhawech-Fauceglia P. *et al.* 2015. Cancer Microenviron.
**2.** Jacob M. *et al.* 2012. Curr. Mol. Med.
**3.** Mariathasan S. *et al.* 2018. Nature
**4.** Domen A. *et al.* 2021. Cancers
**5.** Joshi RS. *et al.* 2021. Cancers
**6.** Niedermeyer J. *et al.* 2001. Int J Dev.
**7.** Kratochwil C. *et al.* 2019. J. Nucl. Med.

## Disclosures

**R.M. Hallett:** POINT Biopharma Inc. **S.E. Poplawski:** Bach Biosciences. **K.E. Novakowski:** POINT Biopharma Inc. **M.H. Dornan:** POINT Biopharma Inc. **S. Ahn:** None. **S. Pan:** Bach Biosciences. **W. Wengen:** Bach Biosciences. **L. Yuxin:** Bach Biosciences. **D.G. Sanford:** Bach Biosciences. **V.S. Hergott:** POINT Biopharma Inc. **Q. Nguyen:** None. **A.P. Belanger:** None. **J.H. Lai:** Bach Biosciences. **W. Bachovchin:** Bach Biosciences; Avacta; POINT Biopharma Inc. **J.A.B. McCann:** POINT Biopharma Inc.

CONTENT OF THIS PRESENTATION IS THE PROPERTY OF THE AUTHOR, LICENSED BY SNMMI. PERMISSION REQUIRED FOR REUSE.